IOP Conference Series: Materials Science and Engineering

Negative thermal expansion of ScF_3: first principles vs empirical molecular dynamics

IOP Conf. Series: Materials Science and Engineering **503** (2019) 012001 doi:10.1088/1757-899X/503/1/012001

Negative thermal expansion of ScF_3: first principles vs empirical molecular dynamics

Dmitry Bocharov[1], Yuri Rafalskij[1], Matthias Krack[2], Mara Putnina[1] and Alexei Kuzmin[1]

[1]Institute of Solid State Physics, University of Latvia, Kengaraga street 8, LV-1063 Riga, Latvia
[2]Paul Scherrer Institut, Forschungsstrasse 111, 5232 Villigen PSI, Switzerland

E-mail: bocharov@latnet.lv

Abstract. The crystal lattice of cubic scandium fluorine (ScF_3) exhibits negative thermal expansion (NTE) over a wide range of temperatures from 10 K to 1100 K. Here the NTE effect in ScF_3 is studied using atomistic simulations based on empirical and *ab initio* molecular dynamics (AIMD) in the isobaric-isothermal (NpT) ensemble. The temperature dependence of the average lattice constant, the Sc–F–Sc bond angle distribution and the radial distribution functions were obtained. Crossover from the NTE to positive thermal expansion occurring at about 1100 K is reproduced by AIMD simulations in agreement with the known experiment data. At the same time, empirical MD model fails to reproduce the NTE behaviour and suggests an expansion of the ScF_3 lattice with increasing temperature. However, both MD models predict strong anisotropy of fluorine atom thermal vibration amplitude, being larger in the direction orthogonal to the Sc–F–Sc atom chain.

1. Introduction

Materials with a negative thermal expansion (NTE) coefficient were known since the beginning of the twentieth century but attracted the wider attention of researchers recently [1, 2, 3, 4]. The control of thermal expansion of materials is important in the technological areas, where the control of the volume of equipment components with high precision or the invariability of material volume with a change in temperature is required. This task can be solved, for example, by combining materials with positive and negative coefficients of thermal expansion (CTE). Possible areas of applications include electronics, fibre optics, astronomical and optical devices, dental prosthesis, etc [5].

Scandium fluoride (ScF_3) is remarkable among NTE materials due to it exhibits NTE properties in a very wide temperature range from 10 K to 1100 K and has isotropic and high CTE values [6]. Note that a structurally similar ReO_3 compound posses NTE effect with a very small CTE and below room temperature [7]. Unlike many other NTE materials as, for example, ZrW_2O_8, HfW_2O_8 [8] or $ZrV_{2-x}P_xO_7$ [9], ScF_3 has simple ABO_3 perovskite-like cubic lattice ($Pm\bar{3}m$ space group) with the A-site being empty that makes it a useful model object for studying NTE mechanism [10, 11, 12, 13, 14].

Possible mechanisms of the NTE effect were reviewed recently [2, 3, 4] and may have structural and electronic origin. Structural NTE is driven by transverse vibrational motion of the polyhedral units as happens in the case of ScF_3, whose structure is built-up by ScF_6

octahedra connected by vertices. Recently, Lasar et al. [15] showed that *ab initio* molecular dynamics (AIMD) can be used to model the NTE effect in ScF_3. They were able to reproduce temperature dependence of the reduced lattice constant, re-normalized at 200 K, using very small $2a_0 \times 2a_0 \times 2a_0$ (a_0 is the lattice constant of ScF_3) supercell.

In this study, we compare the results of empirical MD and AIMD simulations of ScF_3 performed for large supercells with the aim to check the limits of applicability of the two methods for a description of the NTE effect.

2. Computational details

AIMD simulations based on Kohn-Sham density functional theory (DFT) [16] with exchange-correlation potential PBEsol [17] and empirical MD simulations using the Born–Mayer potential [18, 19] were performed in the isobaric-isothermal (NpT) ensemble at seven different temperatures in the range of 300-1600 K using the CP2K code [20].

The equilibrium lattice constant of ScF_3 at T=0 K obtained from preliminary DFT calculations for optimized structure a_0=4.027 Å. The AIMD potential parameters were described previously in [21]. The Born–Mayer interatomic potential was used in empirical MD calculations

$$U(r) = A \exp(-r/B) \tag{1}$$

where A and B are potential parameters (A=942.4541 eV and B=0.2830 Å for the F–F atom pairs, whereas A=10173.51 eV and B=0.2003 Å for Sc–F atom pairs). No interaction between Sc atoms was considered. The potential parameters were optimized by fitting to the lattice constant and comparing the phonons given by this potential with phonon calculated in the Ref. [22]

The initial equilibration run was for both empirical MD and AIMD was 15 ps, followed by the production run of 50 ps. The Newton's equations of motion were integrated with the Verlet leapfrog algorithm, with a time step of 0.5 fs.

The temperature were controlled using the Nosé–Hoover thermostat. Sets of atomic configurations were generated during the MD simulations performed for $5a_0 \times 5a_0 \times 5a_0$ supercells with 500 atoms and used further to calculate the lattice constants a_0 (Fig. 1), the radial distribution functions (RDFs) Sc–F and Sc–Sc (Fig. 2) and the bond angle distribution functions (BADFs) Sc–F–Sc (Fig. 3).

3. Results and discussion

Temperature dependencies of the lattice constant a_0 obtained from empirical MD and AIMD simulations are compared with the experimental diffraction data from [6] in Fig. 1. The AIMD results reproduce the NTE effect in ScF_3 and agree well with the experimental data, overestimating only slightly (less than 0.01 Å) the absolute values of the experimental lattice constant. On the contrary, empirical MD predicts strong positive expansion of the lattice being always above both the experimental and AIMD data.

The difference in the behaviour of lattice constants for two simulation methods is also visible in the RDFs $G(r)$ in Fig. 2, where the RDF peaks obtained by empirical MD are slightly shifted to larger distances. However, both MD simulations predict anharmonic Sc–F bonding, leading to the visible asymmetry of the first peak in the RDFs at 2 Å. This result supports the importance of anharmonic effects in ScF_3 [10].

Finally, the temperature dependencies of the average bond angle Sc–F–Sc between two nearest ScF_6 octahedra are shown in Fig. 3. Note that there is a principal difference between the average bond angle Sc–F–Sc calculated from the instantaneous atomic coordinates, which deviates always from 180° due to transverse atom motion, and the Sc–F–Sc angle calculated from the average atomic positions, which is equal to 180° in cubic ScF_3. As one can see, an increase of temperature

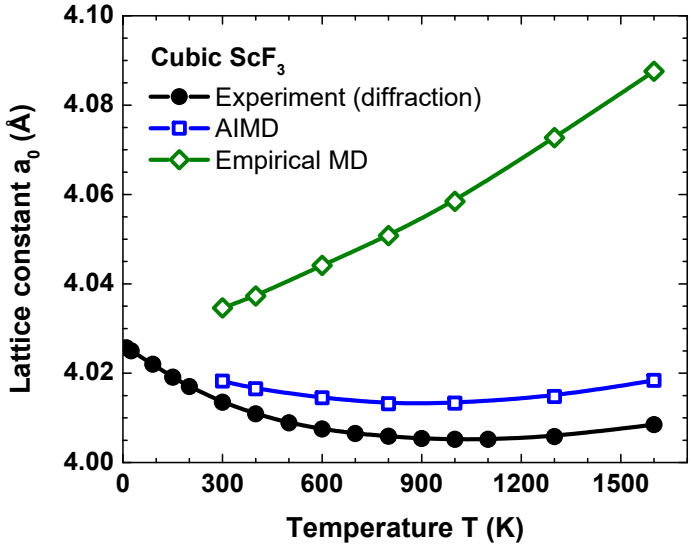

Figure 1. Temperature dependence of the lattice constant a_0 of cubic ScF_3 obtained from empirical MD and AIMD simulations in the NpT ensemble in comparison with the experimental data from [6].

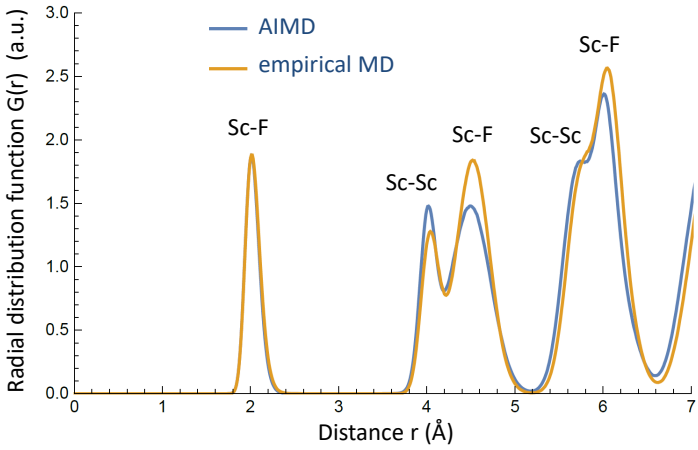

Figure 2. The total radial distribution functions $G(r)$ for Sc–F and Sc–Sc atom pairs at 600 K calculated using the results of the empirical MD and AIMD simulations in the NpT ensemble.

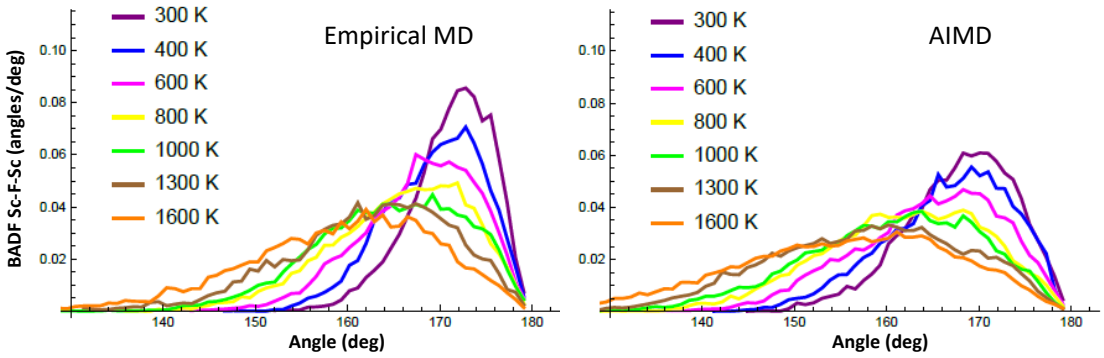

Figure 3. The inter-octahedral Sc–F–Sc bond angle distribution function calculated using the results of the empirical MD and AIMD simulations in the NpT ensemble.

leads to the broadening of BADF and its maximum shifts to smaller angles due to an increase of the amplitude of transverse vibrational motion of fluorine atoms. This effect is observed in

both empirical MD and AIMD simulations. However, the Sc–F–Sc BADFs obtained by AIMD are always broader than those from empirical MD and extend to smaller angular values. This suggests slightly larger vibration amplitude of atoms in the AIMD simulations.

4. Conclusions

Ab initio and empirical molecular dynamics simulations of cubic ScF_3 were performed in the NpT ensemble and using large $5a_0 \times 5a_0 \times 5a_0$ supercells in the temperature range of 300-1600 K. Both simulations predict anharmonic nature of the Sc–F bonds and large amplitude of fluorine atoms transverse motion, which increases at higher temperatures. The negative thermal expansion of the ScF_3 lattice is well reproduced only by *ab initio* MD simulations, which predict the lattice constant values close to those obtained experimentally by diffraction in [6] and a crossover of thermal expansion from negative to positive around 1100 K upon increasing temperature. Empirical MD simulations fail to predict the NTE effect and shows only positive expansion.

Acknowledgments

The calculations were performed on the Paul Scherrer Institute cluster Merlin4, HPC resources of the Swiss National Supercomputing Centre in Lugano (project ID s626) as well as at the Latvian SuperCluster (LASC). Authors are greatly indebted to S. Ali, D. Gryaznov, R.A. Evarestov, M. Isupova, A. Kalinko, V. Kashcheyevs, V. Pankratov, S. Piskunov, A. I. Popov, J. Purans, F. Rocca, L. Shirmane, P. Žguns, and Yu. F. Zhukovskii for many stimulating discussions. Financial support provided by project No. 1.1.1.2/VIAA/l/16/147 (1.1.1.2/16/I/001) under the activity "Post-doctoral research aid" realized at the Institute of Solid State Physics, University of Latvia is greatly acknowledged.

References

[1] Lind C 2012 *Materials* **5** 1125–1154
[2] Dove M T and Fang H 2016 *Rep. Prog. Phys.* **79** 066503
[3] Mittal R, Gupta M and Chaplot S 2018 *Prog. Mater. Sci.* **92** 360–445
[4] Attfield J P 2018 *Front. Chem.* **6** 371
[5] Ventura G and Perfetti M 2014 *Thermal Properties of Solids at Room and Cryogenic Temperatures* (Springer)
[6] Greve B K, Martin K L, Lee P L, Chupas P J, Chapman K W and Wilkinson A P 2010 *J. Am. Chem. Soc.* **132** 15496–15498
[7] Dapiaggi M and Fitch A N 2009 *J. Appl. Crystallogr.* **42** 253–258
[8] Evans J S O, Mary T A, Vogt T, Subramanian M A and Sleight A W 1996 *Chem. Mater.* **8** 2809–2823
[9] Korthuis V, Khosrovani N, Sleight A W, Roberts N, Dupree R and Warren W W J 1995 *Chem. Mater.* **7** 412–417
[10] Piskunov S, Žguns P A, Bocharov D, Kuzmin A, Purans J, Kalinko A, Evarestov R A, Ali S E and Rocca F 2016 *Phys. Rev. B* **93** 214101
[11] van Roekeghem A, Carrete J and Mingo N 2016 *Phys. Rev. B* **94** 020303
[12] Bocharov D, Zguns P, Piskunov S, Kuzmin A and Purans J 2016 *Low Temp. Phys.* **42** 556–560
[13] Hu L, Chen J, Sanson A, Wu H, Guglieri Rodriguez C, Olivi L, Ren Y, Fan L, Deng J and Xing X 2016 *J. Am. Chem. Soc.* **138** 8320–8323
[14] Occhialini C A, Handunkanda S U, Curry E B and Hancock J N 2017 *Phys. Rev. B* **95** 094106
[15] Lazar P, Bučko T and Hafner J 2015 *Phys. Rev. B* **92** 224302
[16] Kohn W and Sham L J 1965 *Phys. Rev.* **140** A1133–A1138
[17] Perdew J P, Burke K and Ernzerhof M 1996 *Phys. Rev. Lett.* **77** 3865–3868
[18] Born M and Mayer J E 1932 *Eur. Phys. J. A* **75** 1–18
[19] Buckingham R A 1938 *Proc. R. Soc. London Ser. A* **168** 264–283
[20] CP2K developers group 2000–2018 (http://www.cp2k.org)
[21] Bocharov D, Krack M, Kalinko A, Purans J, Rocca F, Ali S E and Kuzmin A 2016 *J. Phys.: Conf. Ser.* **712** 012009
[22] Li C W, Tang X, Muñoz J A, Keith J B, Tracy S J, Abernathy D L and Fultz B 2011 *Phys. Rev. Lett.* **107** 195504

Institute of Solid State Physics, University of Latvia as the Center of Excellence has received funding from the European Union's Horizon 2020 Framework Programme H2020-WIDESPREAD-01-2016-2017-TeamingPhase2 under grant agreement No. 739508, project CAMART²